Quadri-Histogram Equalization for infrared images using cut-off limits based on the size of each histogram

Rubén Darío Medina Caballero[a], Isidro Augusto Brizuela Pineda[a], Julio César Mello Román[a], José Luis Vázquez Noguera[a], Juan José Cáceres Silva[b,*]

[a]*Polytechnic School, National University of Asuncion*
[b]*Department of Computer Science, Royal Holloway, University of London*

Abstract

In infrared images, the pixels representing the objects are hidden in a large number of background pixels with low contrast. Several effective contrast enhancement techniques exist in the state of the art today, however they cause the noise level added to the images to increase. The improvement of contrast is an indispensable procedure for the analysis of infrared images, due to the scarce temperature difference between the objects and the background, captured by the surveillance systems using infrared sensors. Therefore, a contrast enhancement algorithm for infrared imaging based on histogram equalization using clipping is presented in this article. The proposed algorithm divides the histogram into 4 subhistograms, then each subhistogram is modified with a cut limit based on the size of the subhistogram in order to limit the improvement of the contrast. The experimental results prove that the algorithm improves the contrast of infrared images by 99%, especially the contrast between the objects and the background of the infrared images preserving the mean brightness and decreasing the aggregate noise level of them. With the proposed algorithm, the background of the infrared image is restricted while the objects are visually contrasted.

Keywords: Contrast enhancement, Clipping, Histogram Equalization, Mean brightness

1. Introduction

In general, the infrared images have a low contrast but a highly blurred background, so the detail information of the objects is easily hidden in the background, making it difficult to distinguish the object from the background [1–4]. This is because the infrared image sensor is sensitive to the variation of the temperature of the image, affecting the quality of the images obtained and blurring the regions of interest in the infrared image. The gray values of the regions of interest are bright or dark, which do not differ from the regions around them. Therefore, the improvement in the infrared image is very important and necessary.

In order to improve the contrast of infrared images [5–11], the dynamic range of gray levels of the image needs to be extended. Although contrast enhancement techniques efficiently increase the contrast level of images, the common issue they have is that they make the background noise of the image be amplified while the details of the objects are restricted. In other words, they mostly produce a high image distortion by adding an important level of noise to the image, making it hard to watch the objects details clearly, they also excessively alters the average brightness of the images and increases the index of fuzziness causing the images to be more confusing and obtain an unnatural aspect.

In the literature there are several contrast enhancement techniques based on histogram equalization [12–18] designed to improve the image contrast level, often at the cost of brightness preservation or signal to noise ratio. Another group of techniques use gamma-based correction to improve contrast [19–21], and exhibit a trade-off similar to histogram equalization methods.

This paper proposes an improved version of the method BPCLBHE [17] called Quadri-Histogram Equalization with Limited Contrast for Infrared Images (QHELC-IR), such that the level of noise added can be minimized and the average brightness is better preserved. The algorithm can be used in applications of surveillance camera systems and automobiles to improve the contrast of infrared images effectively. Among contrast enhancement methods for infrared images there is a technique called IRHE2PL and proposed by Kun Liang et al. [4], which is one of the techniques whose results we compare to the proposed QHELC-IR results.

The article is organized as follows, in the Section 2 is presented and discussed about the QHELC-IR. The experimental results are presented in the Section 3 and the Section 4 presents the conclusion of the work.

*Corresponding author
Email addresses: rdmedina@pol.una.py (Rubén Darío Medina Caballero), iabrizuela@pol.una.py (Isidro Augusto Brizuela Pineda), juliomello@pol.una.py (Julio César Mello Román), jlvazquez@pol.una.py (José Luis Vázquez Noguera), Juan.CaceresSilva.2014@live.rhul.ac.uk (Juan José Cáceres Silva)

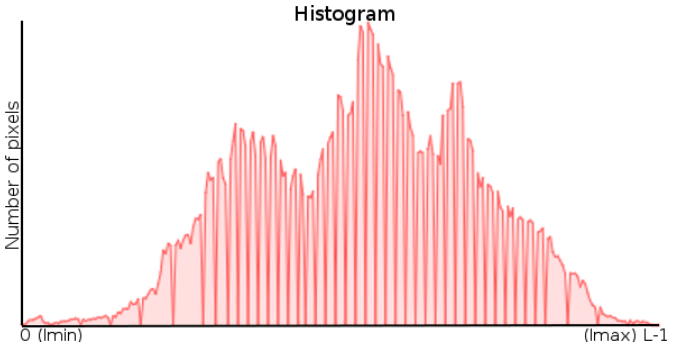

Figure 1: Global histogram of a random image.

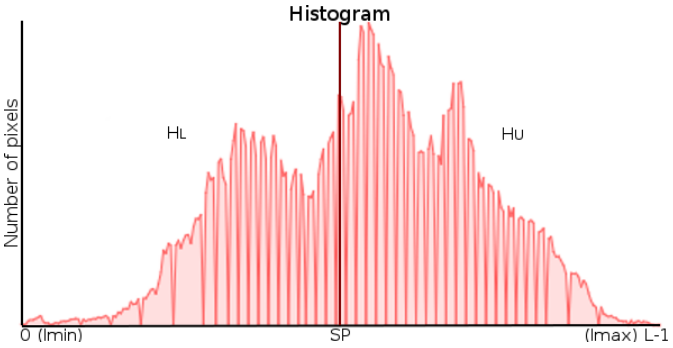

Figure 2: Global histogram after the first division.

2. Quadri-Histogram Equalization with Limited Contrast for Infrared Images

BPCLBHE uses two techniques to improve contrast. The first technique is the segmentation of the histogram using the mean threshold, which leads to the preservation of the mean brightness. The second technique is the histogram clipping, which entails maximizing the entropy to control the contrast enhancement rate. In the proposed method, the clipping and equalization of the histogram are performed in 4 segments to obtain a better preservation of average brightness while minimizing the contrast enhancement. This is achieved by first dividing the global histogram into 2 subhistograms, the lower subhistogram and the upper subhistogram. Then the lower and upper subhistograms are again divided into two subhistograms, thus segregating the histogram into 4 parts.

We think of the process of dividing the histogram into two parts as a simple procedure to independently equalize the foreground and the background of the image. Despite the fact that histograms do not provide a topological mapping for the pixel intensities, several approaches have used histogram thresholding to segment images [31–33]. These methods focus on a simple idea: in order for the background and foreground images to be distinguishable, one must be lighter and the other darker. To illustrate, we can assume that both image sections, background and foreground, come from Gaussian distributions [32]. Naturally, this approach converts the histogram to a mixture of Gaussians, where proper segmentation implies a fuzzy classification of the intensities [31]. However, the usage of a hard threshold is sufficient to improve simultaneously the contrast of the background and foreground of the image as shown by several methods in the literature [22–25] that use bi-histogram equalization to enhance the contrast of the image while preserving the brightness.

Our idea is that we can take this procedure one step further: split the background into a *background-background* and a *background-foreground*, and the foreground into a *foreground-background* and *foreground-foreground*. The additional division aims to allow a better preservation of brightness, while maintaining the potential to improve the image contrast. Following this reasoning, the number of partitions are the different powers of 2 and the next step would require eight windows, which would only allow a minimal improvement in contrast.

Using the histogram as the input space, each pixel is an element which lives in a 1-D space. Therefore, following the interpretation of the image as a mixture of Gaussians, we should be able to identify clusters of pixel intensities, which represent each Gaussian in the mixture. Pixels clustered around the mean colors within the histogram will belong to each image section: background and foreground. We perform the clustering with the well known k-means algorithm [26] (for more details see Section 3.2).

The first step of our proposal is to calculate the threshold SP in the global image histogram by using the k-means algorithm, where the centroids are initialized with the mean histogram value. Then, the histogram is separated into two subhistograms, the lower subhistogram HL, and the upper subhistogram H_U. The subhistogram H_L contains the values of intensities that are found from the minimum level of gray in the image l_{MIN} up to SP, while the subhistogram H_U contains the intensities values that are from $SP1 + 1$ up to the maximum level of gray in the image l_{MAX}. In Figure 1 a graphic example of a global histogram of an image is shown and in Figure 2 the global histogram after the first segmentation is illustrated. The lowest effective intensity within the image is l_{MIN}, that is, the lowest intensity within the histogram that appears at least once in the image, so l_{MAX} represents the maximum effective intensity found in the image, that is, the greater intensity within the histogram that appears at least once in the image.

Once the lower and upper subhistograms are obtained, the thresholds of both subhistograms are calculated analogously with k-means, where the centroids are initialized with the mean subhistogram value. The lower and upper subhistograms are again separated into two subhistograms using SPL and SPU as cut points, respectively, following the same procedure with which the global histogram was separated. These values serve to separate both subhistograms H_L and H_U in two subhistograms: H_{L1} and H_{L2} on intensity SPL, and H_{U1} and H_{U2} on intensity SPU respectively. Formally, the four subhistograms H_i, with $i \in \{L1, L2, U1, U2\}$ are defined as:

$$H_i = \{H(q) | \, q \in R_i\}, \tag{1}$$

where R_i is the range of intensities of each subinterval, in particular $R_{L1} = [0, SPL]$, $R_{L2} = [SPL + 1, SP]$, $R_{U1} = [SP + 1, SPU]$, and $R_{U2} = [SPU + 1, 255]$, as illustrated in

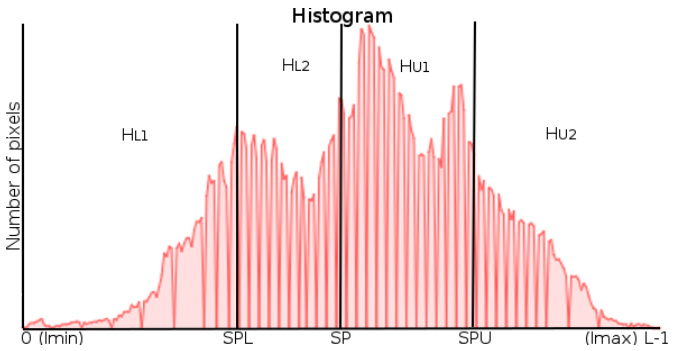

Figure 3: Global histogram after the second division.

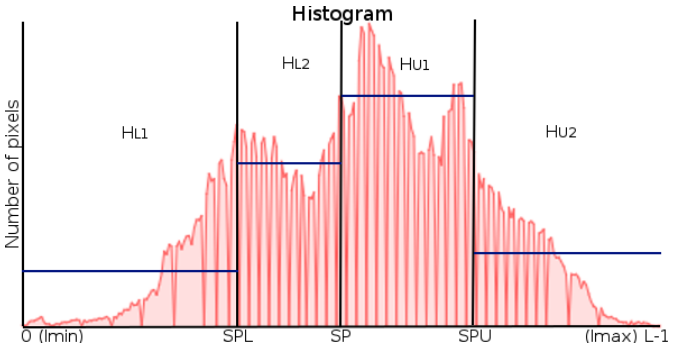

Figure 4: Global histogram with calculated cutting limits.

Figure 3.

To control the over improvement and obtain a natural appearance, we use the trimming technique to modify the 4 subhistograms. Following the ideas from BPCLBHE, we find cut-off limits for each subhistogram, and then redistribute the excess pixels among the other intensities in the subhistogram.

First, we calculate the cut-off limits CL_i (illustrated in Figure 4) as:

$$CL_i = \left\lceil \frac{N_i}{I_i} \right\rceil + round\left(\gamma \times \left(N_i - \frac{N_i}{I_i}\right)\right) \quad (2)$$

where $\lceil\ \rceil$ is the ceil function which rounds up the number to the closest integer, $\gamma \in \mathbb{R}$ with $0 \leq \gamma \leq 1$ is a parameter to control the contrast, I_i is the length of each interval R_i, and N_i is the number of pixels within the subinterval H_i, calculated as:

$$N_i = \sum_{q \in R_i} H_i(q). \quad (3)$$

Then, we compute the total numbers of pixels that exceed the cut-off limit for each level of gray in each subhistogram T_i, as:

$$T_i = \sum_{q \in R_i} max(H_i(q) - CL_i, 0), \quad (4)$$

Next, the average increment AI_i for each level of gray for the subhistogram H_i is calculated as:

$$AI_i = \left\lfloor \frac{T_i}{I_i} \right\rfloor, \quad (5)$$

where $\lfloor\ \rfloor$ is the floor function which rounds down the number to the closest integer.

Finally, we use the cut-off limit CL and the average increase AI to trim each subhistogram and redistribute the excess pixels in each gray level. The trimmed subhistograms H'_i are calculated as:

$$H'_i(q) = \begin{cases} CL_i & \text{if } H_i(q) > CL_i - AI_i \\ H_i(q) + AI_i & \text{otherwise} \end{cases} \quad \forall q \in R_i. \quad (6)$$

Figure 5 illustrates how the histogram remains after being trimmed.

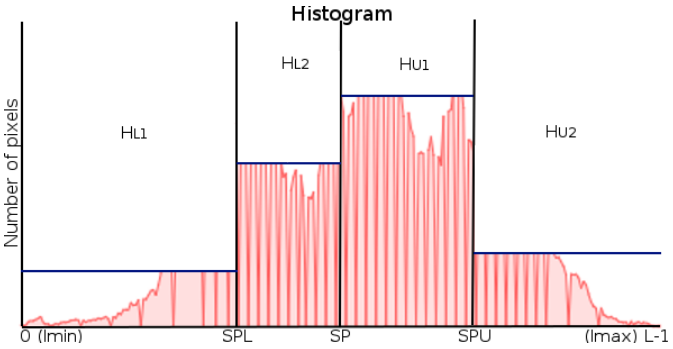

Figure 5: Histogram after the modifications made by the calculated limits.

Once the process of modifying the histogram has finished, we proceed to equalize each trimmed subhistogram independently according to the equation of HE:

$$e_i(q) = X_{inf} + (X_{sup} - X_{inf}) \times c_i(q), q = [X_{inf}, X_{sup}], \quad (7)$$

where e_i is the equalization function that will be used to replace the gray levels in H_i, c_i is the accumulated density function, given by:

$$c_i(q) = \sum_{j=X_{inf}}^{q} p_i(j), \quad (8)$$

where p_i is the probability of occurrence of the intensity of gray q in H'_i, calculated as:

$$p_i(q) = \frac{H'_i(q)}{N_i}, \quad (9)$$

X_{inf} and X_{sup} are the upper and lower limits of the subhistogram range, respectively, and q is the gray level.

Algorithm 1 describes in summary the procedure of the proposed method. It receives the image to be improved and the value for the parameter γ, which will be used as input data, and returns an improved resulting image in contrast.

The following section presents the experimental results, carrying out a comparative analysis between the existing methods in the state of the art and the proposed method.

3. Experimental Results

In this section, comparative analyzes are presented between the proposed QHELC-IR method and the techniques: the histogram equalization (HE) [14], CLAHE [16], IRHE2PL [4],

Algorithm 1 QHELC-IR

procedure

Step 0: The image f and the value of the γ parameter are received as input data.

Step 1: The H histogram of the f image and the probability density function $p(k)$ associated with H are obtained.

Step 2: We proceed to divide the histogram H using k-means algorithm [26] to obtain the threshold SP, in this way we obtain subhistograms H_L and H_U where the range for H_L goes from 0 to SP and the range for H_U goes from $SP1 + 1$ to $L - 1$.

Step 3: We proceed to divide the subhistogram H_L using the k-means algorithm [26] to obtain the threshold SPL, in this way we obtain the subhistograms H_{L1} and H_{L2} where the range for H_{L1} goes from 0 to SPL and the range of H_{L2} goes from $SPL + 1$ to SP.

Step 4: We proceed to divide the subhistogram H_U using the k-means algorithm [26] to obtain the threshold SPU, in this way we obtain the subhistograms H_{U1} and H_{U2} where the range for H_{U1} goes from $SP + 1$ to SPU and the range of H_{U2} goes from $SPU + 1$ to $L - 1$.

Step 5: We proceed to calculate the values that are used to modify the histogram. This is done for each subhistogram as follows:

1. The cutoff values CL_{L1}, CL_{L2}, CL_{U1} and CL_{U2} are obtained as indicated in Equation (2). For subhistograms H_{L1} and H_{U1}, cutoff limits CL_{L1} and CL_{U1} are used, respectively. For the subhistograms H_{L2} and H_{U2} we use CL_{L2} and CL_{U2}, correspondingly.
2. The total numbers of pixels which exceed the cutoff limit T is calculated as indicated in Equation (4). Note that this is calculated for each level of gray in each subhistogram.
3. The average increments AI per subhistogram are calculated as indicated by Equation (5). The T values calculated above are used.

Step 6: The H histogram is modified as H' using Equation (6) for all four subhistograms.

Step 7: Once the histogram is modified, we proceed to equalize H_{L1}, H_{L2}, H_{U1} and H_{U2} with Equation (7). This function will be used to replace the intensities of the original image in order to obtain the equalized image f'.

AGCWD [19], IEGAGC [20] and BPCLBHE [17]. Seven metrics were used to determine the validity of the proposed algorithm. They are:

1. The contrast [27] is defined as:

$$C = \sqrt{\sum_{q=0}^{L-1}(q - E(f))^2 \times p(q)}, \tag{10}$$

where $E(f)$ represents the mean brightness of the image. When the value of the contrast of the result image $E(f')$ is greater than the value of the contrast of the input image, then there is an improvement.

2. Absolute Mean Brightness Error (AMBE) [28], which measures the alteration of the average brightness of the image, is given by the equation:

$$AMBE = |E(f) - E(f')|, \tag{11}$$

where f and f' represent the input image and the result image, respectively, $E(f)$ and $E(f')$ represent the average brightness of the input image and the result image, respectively . The smaller the value of the AMBE, the better is the preservation of the brightness of the image.

3. The Contrast/Original Contrast Ratio (CR): This metric measures whether the initial contrast of an image is improved. If the value is greater than 1, then the image obtained an increase in contrast.
4. The AMBE to Contrast/Original Contrast Ratio (A/CR): This metric quantifies the distortion of the average brightness needed for a given improvement in contrast. The lower the value, the better the preservation of the average brightness.
5. The execution time of the method, it is given in milliseconds.
6. Peak Signal to Noise Ratio (PSNR) [29], given an input image $f(i, j)$ of $M \times N$ pixels and a reconstructed image $f'(i, j)$, indicates the signal-to-noise ratio of f' compared to f . The PSNR is given by:

$$PSNR = 10\log_{10}\left[\frac{(L-1)^2}{MSE}\right], \tag{12}$$

where the Mean Squared Error (MSE) is given by:

$$MSE = \frac{\sum_{i=1}^{M}\sum_{j=1}^{N}[f(i,j) - f'(i,j)]^2}{M \times N} \tag{13}$$

The higher the value of the PSNR, the lower the noise introduced in the image, and therefore the quality of the resulting image is not affected.

7. The linear index of fuzziness is based on the analysis of spatial domain, it has been widely used to quantitatively compare the improvement performance of different algorithms. The ambiguity in an image is measured with this index denoted by γ and defined as:

$$\delta(f) = \frac{2}{M \times N}\sum_{i=1}^{M}\sum_{j=1}^{N} min(r(i,j), (1 - r(i,j))), \tag{14}$$

$$r(i,j) = \sin(\frac{\pi}{2} \times (1 - \frac{f(i,j)}{f_{max}})), \tag{15}$$

where $f(i, j)$ and f_{max} represent the gray level of the pixel (i, j) and the maximum gray level of an image f with size $M \times N$, respectively. The smaller the value of δ, the better the performance of the image improvement.

The experiments that compose this section are:

- In subsection 3.1, Experiment 1, which analyses the AMBE, the Contrast/Original Contrast Ratio and the AMBE to Contrast/Original Contrast Ratio for different values of contrast that the proposed technique and BPCLBHE can produce, varying the value of γ. The objective is to identify the behaviour of the mean brightness for each level of contrast.

- In subsection 3.2, Experiment 2, which compares different clustering methods to segment the histogram found in the literature. We consider Contrast, AMBE and execution time as evaluation metrics. The aim is to determine which method has the best performance considering the metrics mentioned above and the complexity of each method.

- In subsection 3.3, Experiment 3, which compares QHELC-IR with other techniques of the literature, considering time, contrast, AMBE, PSNR and Fuzziness as evaluation metrics. The aim is to determine the level of competitiveness of the proposed method in each of these metrics and the advantages it has over other techniques.

For these experiments we used the public database ICRA 2014 - Thermal Infrared Dataset [30]. The dataset contains 100 8-bit images, all equal in size (324 × 256 px). The algorithms were implemented in ImageJ version 1.48 and were executed on a personal computer with Intel Core i3-M350 processor of 2.27 GHz, 4 GB of RAM and Ubuntu 14.04 LTS 64 bits operating system.

3.1. Experiment 1: Sensitivity analysis of the contrast

In this experiment, we produce a comparative analysis of AMBE, Contrast/Original Contrast Ratio, and the AMBE to Contrast/Original Contrast Ratio for a range of contrast enhancements given by varying the γ parameter from 0 to 1 in both techniques: QHELC-IR and BPCLBHE.

Table 1 shows different contrast levels that can be reached by QHELC-IR and BPCLBHE. Both methods tends to increment the CR value by increasing the γ parameter from 0 to 1. There is an overlap between the ranges of the produced contrast levels where we could compare and analyze the other metrics for both methods. We can see that QHELC-IR has a better performance than BPCLBHE in terms of A/CR, which means that QHELC-IR adds less distortion to the images than BPCLBHE by producing virtually the same contrast levels. Also, while the QHELC-IR technique reaches smaller contrast levels and thus it gets better AMBE values, the BPCLBHE technique obtains higher contrast improvements and makes the images lose more natural brightness.

QHELC-IR					BPCLBHE				
γ	C	A	CR	A/CR	γ	C	A	CR	A/CR
0	43.24	0.74	1.04	0.71	-	-	-	-	-
0.001	44.05	1.07	1.06	1.01	-	-	-	-	-
0.0024	45.17	1.54	1.09	1.41	-	-	-	-	-
0.0038	46.28	2.01	1.11	1.80	-	-	-	-	-
0.0048	47.06	2.34	1.13	2.07	-	-	-	-	-
0.006	47.99	2.73	1.16	2.36	0	47.53	2.87	1.14	2.51
0.008	49.49	3.37	1.19	2.82	0.0005	49.05	3.71	1.18	3.14
0.009	50.21	3.68	1.21	3.04	0.0008	49.94	4.20	1.20	3.49
0.01	50.88	3.96	1.23	3.23	0.001	50.51	4.52	1.22	3.71
0.012	52.15	4.48	1.26	3.57	0.0015	51.88	5.28	1.25	4.22
0.014	53.28	4.95	1.28	3.86	0.002	53.19	5.99	1.28	4.68
0.015	53.77	5.16	1.29	3.98	0.0024	54.19	6.54	1.31	5.01
0.018	55.12	5.71	1.33	4.30	0.0027	54.91	6.95	1.32	5.25
0.02	55.88	6.02	1.35	4.47	0.003	55.59	7.32	1.34	5.47
0.024	57.12	6.51	1.38	4.73	0.0038	57.30	8.25	1.38	5.98
0.026	57.64	6.72	1.39	4.84	0.004	57.70	8.47	1.39	6.09
0.03	58.53	7.09	1.41	5.03	0.0048	59.16	9.30	1.42	6.52
0.04	60.11	7.75	1.45	5.35	0.005	59.52	9.50	1.43	6.63
1	61.13	8.63	1.47	5.86	0.006	61.13	10.43	1.47	7.08
-	-	-	-	-	0.0068	62.29	11.11	1.50	7.40
-	-	-	-	-	0.007	62.55	11.25	1.51	7.47
-	-	-	-	-	1	73.38	19.53	1.77	11.05

Table 1: Averages of Contrast (C), AMBE (A), CR and A/CR

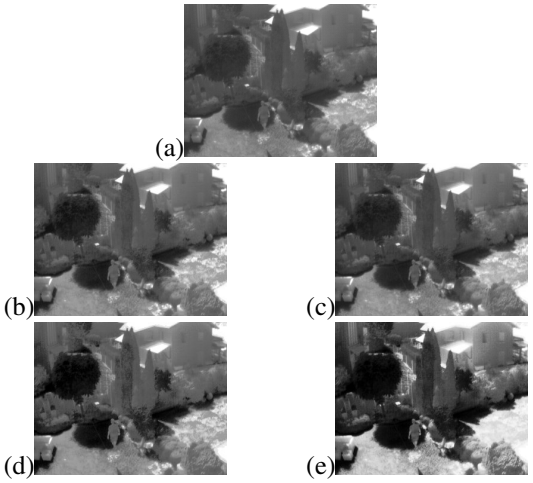

Figure 6: Image 63 from the public database and its respective equalizations. (a) Original, (b) QHELC-IR with γ=0.006, (c) BPCLBHE with γ=0, (d) QHELC-IR with γ=1, (e) BPCLBHE with γ=1.

Figure 6 shows an image from the database equalized with QHELC-IR and BPCLBHE. Subfigures (b) and (c) are the image equalized by QHELC-IR with γ=0.006 and the comparable image equalized by BPCLBHE with γ=0, respectively. It can be seen that the grass on the right side of the image equalized with BPCLBHE blends into the background more than the grass in the image equalized with QHELC-IR. This blending gets more evident in the images equalized with γ=1, which produces a higher contrast level for both methods. QHELC-

IR method keeps the natural appearance in a better way even when the alteration is the highest.

3.2. Experiment 2: Histogram partitioning methods

Previous authors have used statistic measures to divide the histogram into two regions (in particular the average intensity [22, 23]). Our approach adds in this step the versatility of a clustering technique to separate the histogram into naturally occurring groups of intensities. This allows a better segmentation of the histogram in case of an imbalance of light-dark pixels.

The following experiment aims to analyze the benefits and drawbacks of several well-known clustering methods. We compare the usage of k-means [26], Expectation Maximization [35], Hierarchical Clustering [36], and finally an extension of the classic k-means known as k-means++ [34]. The k-means algorithm is iterative: in each iteration, elements are assigned to the cluster from closest centroid (which are points from the same space as the elements), and then new centroids are calculated with the average position of each element of the cluster. The algorithm iterates until convergence or a limited amount of steps. The k-means++ algorithm intends to produce well distributed centroids, by selecting centroids iteratively and prioritizes points farther from the already selected centroids. Expectation Maximization is an iterative method that estimates the latent variables of a mixture of Gaussians model using the maximum likelihood estimates. And finally, we use an agglomerative Hierarchical Clustering with a simple Euclidean distance that iteratively combines the clusters with the smallest average pairwise distances, until reaching the desired amount of clusters.

k-means		k-means++		EM		Hierarchical	
C	A	C	A	C	A	C	A
41.38	0.77	41.16	1.10	-	-	-	-
42.22	1.13	41.70	1.36	42.03	1.52	41.78	1.08
43.36	1.63	42.76	1.89	43.05	2.04	42.93	1.60
50.99	4.86	51.03	5.87	50.76	5.79	51.24	5.25
54.17	6.21	54.28	7.70	54.03	7.28	53.92	6.33
59.45	9.05	-	-	59.76	10.15	59.18	8.38
-	-	-	-	-	-	60.70	9.51

Table 2: Contrast (C) and AMBE (A) results averaged for the 84 images of the public database, which were successfully clustered by all methods.

Table 2 shows the average AMBE and Contrast obtained for the different methods, and the range in which they operate. We can see that the AMBE for the k-means method is generally lower than for the other clustering methods, which is the main concern of our proposal (only the Hierarchical Clustering appears directly comparable, k-means++ performs slightly worse, and EM has the lowest performance). Additionally all methods produced comparable fuzziness values, ranging from 0.244 to 0.264 (not shown in the table to avoid clutter). Furthermore, we notice that EM fails to properly divide all histograms into four clusters, thus reducing the size of the experimental setup.

Methods	**Time**	**Images**	**AMBE**		**Contrast**	
	(ms)	(%)	min	max	min	max
k-means	6.098	100	0.77	9.05	41.38	59.45
k-means++	6.090	100	1.10	7.70	41.16	54.28
EM	18811.57	84	1.52	10.15	42.03	59.76
Hierarchical	92496.30	100	1.08	9.51	41.78	60.70

Table 3: Averaged results for the 100 images of the public database

Table 3 shows a summary of Table 2 and additional details about the performance of the clustering algorithms. This shows that k-means not only produces the best results regarding AMBE, but is also a fast classification method in particular when compared to EM or Hierarchical clustering.

Following these results, we consider k-means similar in speed and slightly superior in performance compared to k-means++, similar in performance and very superior in speed when compared to the Hierarchical Clustering, and superior in both measures when compared to EM (which also suffers problems in classification for our purposes). Additionally, we also consider convenient to set k-means as the default clustering method of our proposal to allow easy implementations of our algorithm.

3.3. Experiment 3: Comparison of QHELC-IR with other methods of literature

In this experiment the proposed method was compared with other techniques, in addition to BPCLBHE, existing in the literature: HE, CLAHE, IRHE2PL, AGCWD and IEGAGC.

Methods	**T(ms)**	**AMBE**	**PSNR**	**Fuzziness**	**Contrast**
Original				0.258	41.52
HE	**0.633**	54.226	12.581	0.403	**73.136**
AGCWD	3.16	38.501	14.789	0.350	63.375
CLAHE	954.614	23.18	17.082	0.35	56.94
IRHE2PL	**0.787**	29.343	25.584	0.342	59.153
IEGAGC	23.246	**1.401**	**34.544**	0.263	42.142
BPCLBHE	1.281	2.869	31.336	**0.251**	47.528
		19.53	16.171	0.278	**73.38**
QHELC-IR	6.151	**0.736**	**40.069**	**0.257**	43.236
		8.63	20.596	0.257	61.13

Table 4: Averaged results for the 100 images of the public database. The highlighted numbers represent the top 2 performing algorithms on each measure.

Table 4 shows the average of the metrics of the literature techniques: HE, CLAHE, IRHE2PL, AGCWD, IEGAGC and BPCLBHE, and of the proposed QHELC-IR technique. For the QHELC-IR and BPCLBHE methods, the results of $\gamma = 0$ (top row) and $\gamma = 1$ (bottom row) were taken to illustrate the range of their performance. Furthermore, Tables 5, 6, 7 and 8 contain individual results of five images, of the public database, equalized with the proposal and the literature techniques mentioned above. Contrast, AMBE, PSNR and Fuzziness results are shown in these tables, respectively.

Methods	Image 15	Image 21	Image 73	Image 78	Image 94
Original	56.87	33.13	28.40	28.87	64.19
HE	**73.56**	**72.85**	**73.51**	**73.01**	**73.36**
AGCWD	**70.10**	**75.61**	**61.68**	**61.30**	63.34
CLAHE	58.34	56.68	55.55	49.67	64.68
IRHE2PL	62.28	66.50	46.51	44.02	**82.50**
IEGAGC	57.03	34.70	29.74	29.33	64.29
BPCLBHE	66.37	40.42	34.16	34.20	69.95
QHELC-IR	59.17	35.19	30.27	30.85	65.60

Table 5: Contrast for particular images of the public database. The highlighted numbers represent the top 2 performing algorithms.

Methods	Image 15	Image 21	Image 73	Image 78	Image 94
HE	4.80	79.38	66.68	87.65	18.28
AGCWD	37.69	49.22	53.28	38.69	22.18
CLAHE	4.27	36.66	39.59	40.49	20.11
IRHE2PL	12.48	54.40	32.62	24.38	33.19
IEGAGC	3.06	**1.20**	**1.55**	**1.36**	**2.65**
BPCLBHE	**2.18**	3.08	1.57	2.82	9.03
QHELC-IR	**0.46**	**0.25**	**0.57**	**0.92**	**0.89**

Table 6: AMBE for particular images of the public database. The highlighted numbers represent the top 2 performing algorithms.

Methods	Image 15	Image 21	Image 73	Image 78	Image 94
HE	20.65	9.08	9.99	8.19	18.44
AGCWD	15.96	11.87	12.15	14.03	19.80
CLAHE	21.27	15.10	14.00	14.48	19.12
IRHE2PL	25.45	12.01	16.69	18.94	16.53
IEGAGC	**30.05**	**33.13**	32.30	**36.19**	29.38
BPCLBHE	28.22	30.13	**32.44**	32.38	**26.98**
QHELC-IR	**37.83**	**40.65**	**40.99**	**40.11**	**37.15**

Table 7: PSNR for particular images of the public database. The highlighted numbers represent the top 2 performing algorithms.

Methods	Image 15	Image 21	Image 73	Image 78	Image 94
HE	**0.40**	0.41	0.40	0.41	0.40
AGCWD	**0.33**	0.28	0.43	0.28	0.40
CLAHE	0.48	0.34	0.39	0.28	0.38
IRHE2PL	0.44	0.34	0.39	0.22	**0.23**
IEGAGC	0.51	**0.141**	**0.183**	**0.100**	0.37
BPCLBHE	0.45	0.16	0.19	0.11	**0.33**
QHELC-IR	0.50	**0.139**	**0.179**	**0.101**	0.36

Table 8: Fuzziness for particular images of the public database. The highlighted numbers represent the top 2 performing algorithms.

The HE and AGCWD methods achieve contrast enhancements higher than the maximum attainable for our method, but they do so by making images much brighter (notice the realy high AMBE values). The HE also adds a significant amount of noise (low PSNR value). CLAHE and IRHE2PL produce a contrast improvements already within the range of our method but add more brightness and noise to the images (see Figure 7). On the other hand, IEGAGC is able to produce a moderate amount of contrast enhancement (less than the minimum produced by our method) for a high preservation in mean brightness (second best after our method). Finally, the techniques BPCLBHE and QHELC-IR, based on histogram clipping, produce a range of results and are able to achieve a moderate improvement in contrast and high preservation of brightness and blur, to higher improvements in contrast at a significant lower cost of brightness and blur compared to the other methods. However, our proposal, QHELC-IR, preserves the mean brightness in a better way because it adds a minimal amount of noise to the images, thus obtaining that the images maintain their naturalness having been improved in terms of contrast.

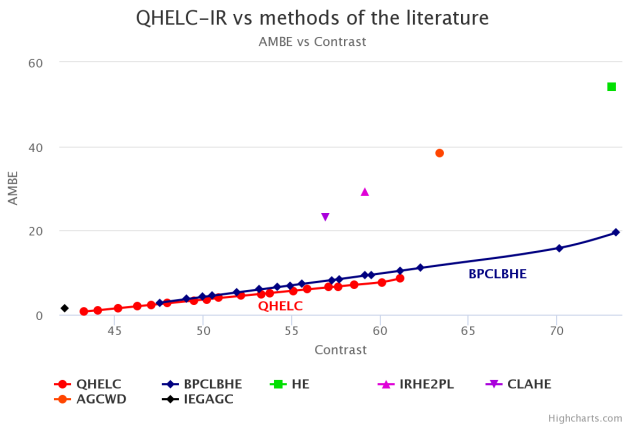

Figure 7: Comparison between AMBE vs Contrast. The points show the average AMBE and Contrast values for the database. The QHELC and BPCLBHE methods are parametric and show several possible combinations.

Figure 7 uses data from Tables 1 and 4, and shows the trade-off between AMBE and Contrast for all the methods. The figure shows the expected increase in brightness alteration (and a decrease in image quality) for a higher improvement in contrast. The best performances are located to the lower right (better AMBE is lower, better contrast is to the right). Thus, each point dominates (is better than) all points located above and to the left in the figure. We can see that QHELC-IR (red) dominates all the other methods throughout its domain. That means that the proposed method obtains the best AMBE to Contrast ratio.

Figures 8 to 12 show excerpts of equalized images from the database to illustrate visual differences between the analyzed methods. We can see that the HE (b) and AGCWD (e) methods overexpose the light details introducing high brightness noise to the image. In particular Figure 12 shows how the HE (b), CLAHE (c) and IRHE2PL (d) give the shadows an unnatural shading. The IEGAGC method (f) adds a frame-like effect around many images which is noticeable in Figure 12 – i.e. the shadow becomes lighter at the bottom and left edges, while no such effect is present in the original (a). We can also notice that BPCLBHE (g) is the most comparable to our method (h), as they both enhance borders and details with minimal distortion to the original image (see Figures 9, 10 and 11). In Figure 8, the

effects of BPCLBHE and our method on the window frame are pretty similar, however BPCLBHE darkens both the plant and the background, while our method keeps the plant with its original color and darkens the background to increase the contrast. We believe that these visual characteristics match the expectations given by our design principles and the numerical results from the previous experiments.

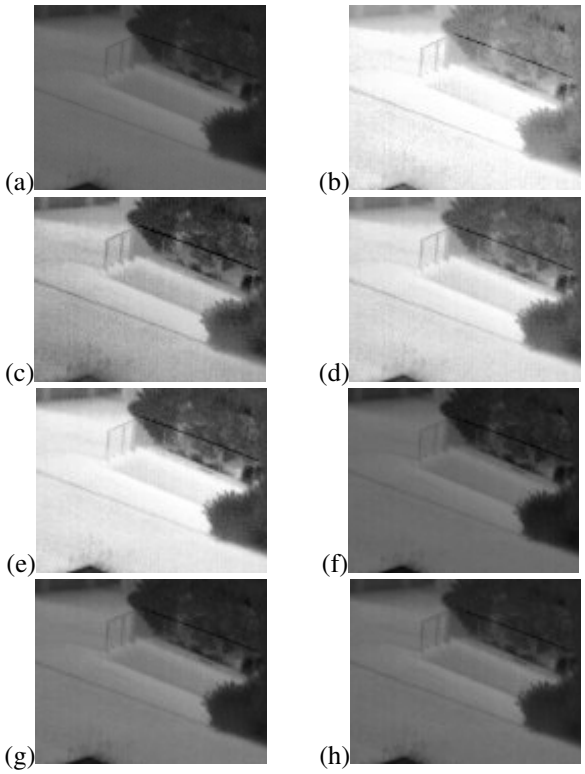

Figure 9: Excerpt from image 21 of the public database and its respective equalizations. (a) Original, (b) HE, (c) CLAHE, (d) IRHE2PL, (e) AGCWD, (f) IEGAGC, (g) BPCLBHE, (h) QHELC-IR.

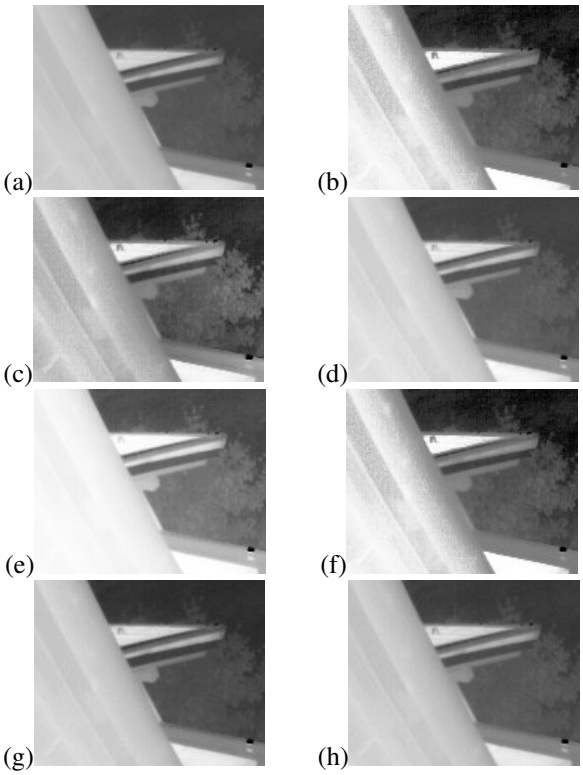

Figure 8: Excerpt from image 15 of the public database and its respective equalizations. (a) Original, (b) HE, (c) CLAHE, (d) IRHE2PL, (e) AGCWD, (f) IEGAGC, (g) BPCLBHE, (h) QHELC-IR.

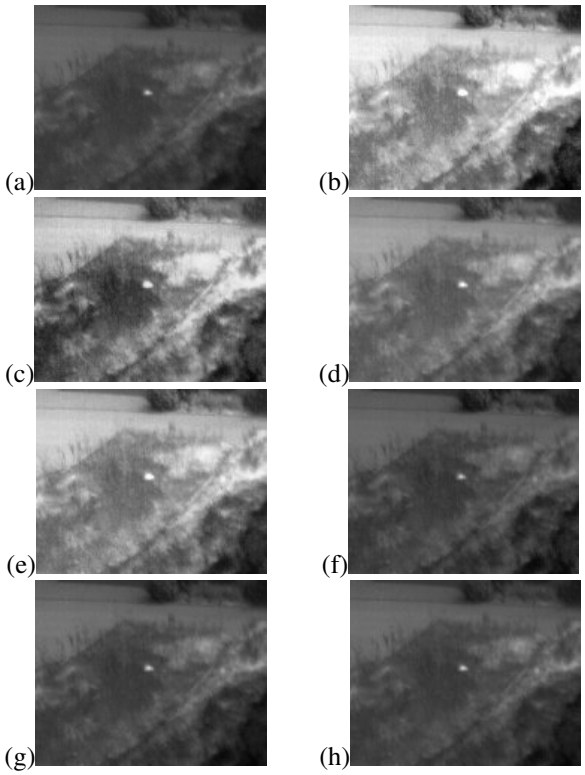

Figure 10: Excerpt from image 73 of the public database and its respective equalizations. (a) Original, (b) HE, (c) CLAHE, (d) IRHE2PL, (e) AGCWD, (f) IEGAGC, (g) BPCLBHE, (h) QHELC-IR.

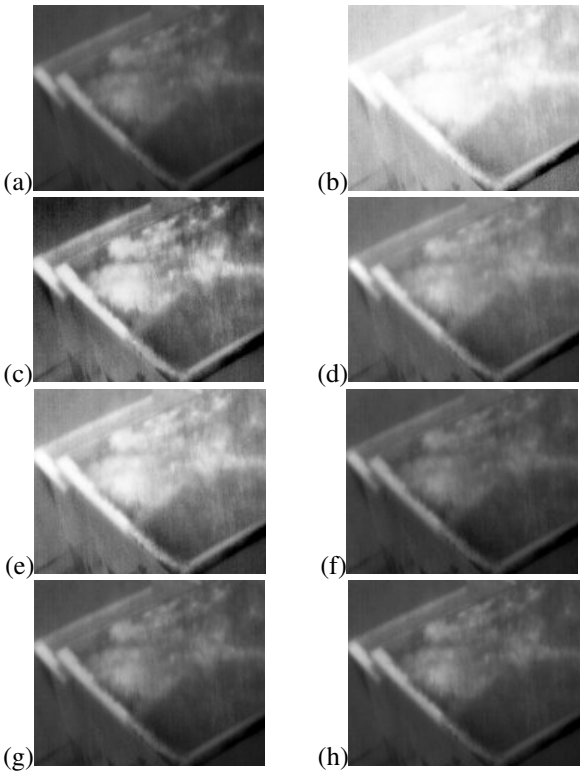

Figure 11: Excerpt from image 78 of the public database and its respective equalizations. (a) Original, (b) HE, (c) CLAHE, (d) IRHE2PL, (e) AGCWD, (f) IEGAGC, (g) BPCLBHE, (h) QHELC-IR.

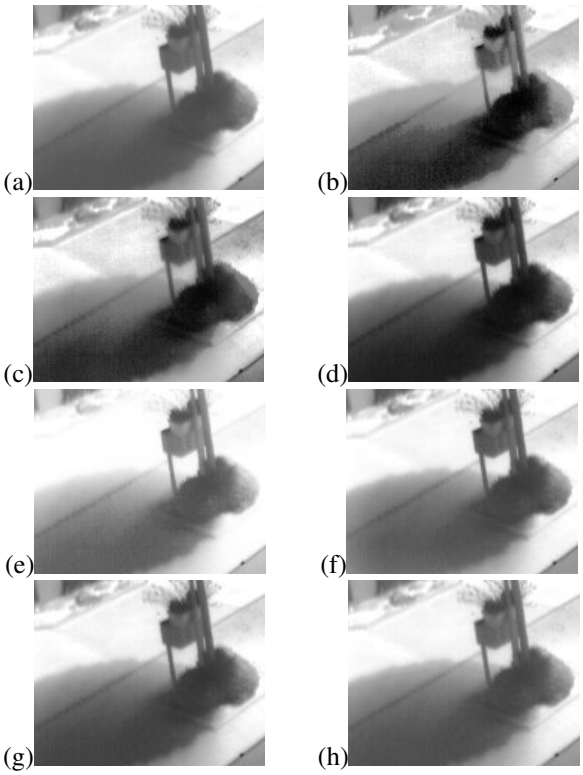

Figure 12: Excerpt from image 94 of the public database and its respective equalizations. (a) Original, (b) HE, (c) CLAHE, (d) IRHE2PL, (e) AGCWD, (f) IEGAGC, (g) BPCLBHE, (h) QHELC-IR.

4. Conclusion

In this work we propose an algorithm of contrast improvement based on the segmentation and clipping of an histogram. The histogram segmentation is efficiently produced by clustering techniques, which allow for natural agglomeration of pixel intensities. The cut-off limits follow a well established paradigm to limit the enhancement on each subhistogram. This algorithm is efficient to improve the contrast and at the same time preserves the average brightness of infrared images.

The experiments based on aerial thermal images show that the AMBE is strongly linked to the improvement of contrast – i.e. the greater the improvement of contrast, the greater the alteration of the mean brightness of the image. In particular, the experiments show that our method obtains a better preservation of mean brightness throughout its operative range when compared to its closest competitor BPCLBHE. We observe that the segmentation and clipping algorithm is able to restrict the background noise while improving the contrast of the image, and we suggest this is the main feature that differentiates our method from others.

In general, the proposed algorithm has a significant contrast enhancement range, and outperforms state-of-the-art methods at preserving the average brightness and reducing the amount of aggregate noise of the infrared images throughout all its contrast range.

References

[1] Chih-Lung Lin, An approach to adaptive infrared image enhancement for longrange surveillance, Infrared Physics and Technology 54 (2) (2011) 84-91.

[2] Carlos Villaseor-Mora, Francisco J. Sanchez-Marin, Maria E. Garay-Sevilla, Contrast enhancement of mid and far infrared images of subcutaneous veins, Infrared Physics and Technology 51 (3) (2008) 221-228.

[3] Rui Lai, Shangqian Liu, Bingjian Wang, Qing Li, A new adaptive enhancement algorithm for infrared image, Semiconductor Optoelectronics 27 (6) (2006) 767-769.

[4] Liang, K., Ma, Y., Xie, Y., Zhou, B., Wang, R.: A new adaptive contrast enhancement algorithm for infrared images based on double plateaus histogram equalization. Infrared Physics and Technology. 55(4), 309-315 (Jul. 2012).

[5] J. C. M. Román, H. L. Ayala and J. L. V. Noguera, "Top-Hat Transform for Enhancement of Aerial Thermal Images", 2017 30th SIBGRAPI Conference on Graphics, Patterns and Images (SIBGRAPI), Niteroi, 2017, pp. 277-284.

[6] Ching-Chung Yang, Image enhancement by adjusting the contrast of spatial frequencies, Optik International Journal for Light and Electron Optics 119 (3) (2008) 143-146.

[7] Xiangzhi Bai, Fugen Zhou, Bindang Xue, Infrared image enhancement through contrast enhancement by using multiscale new top-hat transform, Infrared Physics and Technology 54 (2) (2011) 61-69.

[8] Songfeng Yin, Liangcai Cao, Yongshun Ling, Guofan. Jin, One color contrast enhanced infrared and visible image fusion method, Infrared Physics and Technology 53 (2) (2010) 146-150.

[9] H. Gökhan Ilk, Onur Jane, Özlem Ilk, The effect of Laplacian filter in adaptive unsharp masking for infrared image enhancement, Infrared Physics and Technology 54 (5) (2011) 427-438.

[10] Jin-Hyung Kim, Jun-Hyung Kim, Seung-Won Jung, Chang-Kyun Noh, Sung-Jea Ko, Novel contrast enhancement scheme for infrared image using detail-preserving stretching, Optical Engineering 50 (7) (2011) 077002-1-077002-10.

[11] J.A. Stark, Adaptive image contrast enhancement using generalizations of histogram equalization, IEEE Transactions on Image Processing 9 (5) (2000) 889-896.

[12] S.S. Agaian, B. Silver, K.A. Panetta, Transform coefficient histogram-based image enhancement algorithms using contrast entropy, IEEE Transactions on Image Processing 16 (3) (2007) 741-758.
[13] Qian Chen, Lian-Fa Bai, Bao-Min Zhang, Histogram double equalization in infrared image, Journal of Infrared and Millimeter Waves 22 (6) (2003) 428-430.
[14] H. Ibrahim, N.S.P. Kong, Brightness preserving dynamic histogram equalization for image contrast enhancement, IEEE Transactions on Consumer Electronics 53 (4) (2007) 1752-1758.
[15] K.S. Sim, c.P. Tso, Y.Y. Ta, Recursive sub-image histogram equalization applied to gray scale images, Patter Recognition Letters 28 (10) (2007) 1209-1221.
[16] Pizer, Stephen M., et al. "Adaptive histogram equalization and its variations." Computer vision, graphics, and image processing 39.3 (1987): 355-368.
[17] Yao, Z., Lai, Z., Wang, C., and Xia, W. (2016, November). Brightness preserving and contrast limited bi-histogram equalization for image enhancement. In Systems and Informatics (ICSAI), 2016 3rd International Conference on (pp. 866-870). IEEE.
[18] Pabla B. Aquino Morínigo, Freddy R. Lugo Solís, Diego P. Pinto Roa, Horacio Legal Ayala, José Luis Vázquez Noguera: Bi-histogram equalization using two plateau limits: An International Journal (SIViP). (Dec. 2016).
[19] Huang, Shih-Chia, Fan-Chieh Cheng, and Yi-Sheng Chiu. "Efficient contrast enhancement using adaptive gamma correction with weighting distribution." IEEE Transactions on Image Processing 22.3 (2013): 1032-1041.
[20] Huang, Zhenghua, et al. "Adaptive gamma correction based on cumulative histogram for enhancing near-infrared images." Infrared Physics and Technology 79 (2016): 205-215.
[21] Huang, Zhenghua, et al. "Optical remote sensing image enhancement with weak structure preservation via spatially adaptive gamma correction." Infrared Physics and Technology 94 (2018): 38-47.
[22] Kim, Y.T.: Contrast Enhancement Using Brightness Preserving Bi-Histogram Equalization. IEEE Trans. Consum. Electron. 43(1), 1-8 (Feb. 1997)
[23] Ooi, C.H., Kong, N.S.P., Ibrahim, H.: Bi-histogram equalization with a plateau limit for digital image processing. IEEE Trans. Consum. Electron. 55(4), 2072-2080 (Nov. 2009).
[24] Wang, Y., Chen, Q., Zhang, B.: Image Enhancement Based on Equal Area Dualistic Sub-Image Histogram Equalization Method. IEEE Trans. Consum. Electron. 45(1), 68-75 (Feb. 1999).
[25] Chen, S.D., Ramli, A.R.: Minimum Mean Brightness Error Bi-Histogram Equalization in Contrast Enhancement. IEEE Trans. Consum. Electron. 49(4), 1310-1319 (Nov. 2003).
[26] S. P. Lloyd, Least Squares Quantization in PCM, IEEE Trans. Information Theory, vol. 28, 129-137, 1982.
[27] Lim, S.H., Isa, N.A.M., Ooi, C.H., Toh, K.K.V.:A new histogram equalization method for digital image enhancement and brightness preservation. Springer Signal, Image and Video Processing. (Jun. 2013).
[28] Aedla, R., Siddaramaiah, D.G., Reddy D.V.: A Comparative Analysis of Histogram Equalization based Techniques for Contrast Enhancement and Brightness Preserving. International Journal of Signal Processing, Image Processing and Pattern Recognition. 6(5), 353-366 (2013).
[29] Kandeel, A.A., Abbas, A.M., Hadhoud, M.M., El-Saghir, Z.: A Study Of A Modified Histogram Based Fast Enhancement Algorithm (MHBFE). Signal and Image Processing : An International Journal (SIPIJ). 5(1), (Feb. 2014).
[30] Simon Lynen, Jan Portmann. Thermal Infrared Dataset. https://projects.asl.ethz.ch/datasets/doku.php?id=ir:iricra2014.
[31] Tobias, Orlando Jos, and Rui Seara. "Image segmentation by histogram thresholding using fuzzy sets." IEEE transactions on Image Processing 11.12 (2002): 1457-1465.
[32] Ridler, T. W., and S. Calvard. "Picture thresholding using an iterative selection method." IEEE trans syst Man Cybern 8.8 (1978): 630-632.
[33] Kapur, Jagat Narain, Prasanna K. Sahoo, and Andrew KC Wong. "A new method for gray-level picture thresholding using the entropy of the histogram." Computer vision, graphics, and image processing 29.3 (1985): 273-285.
[34] Arthur, David, and Sergei Vassilvitskii. "k-means++: The advantages of careful seeding." Proceedings of the eighteenth annual ACM-SIAM symposium on Discrete algorithms. Society for Industrial and Applied Mathematics, 2007.
[35] Dempster, Arthur P., Nan M. Laird, and Donald B. Rubin. "Maximum likelihood from incomplete data via the EM algorithm." Journal of the royal statistical society. Series B (methodological) (1977): 1-38.
[36] Schtze, Hinrich, Christopher D. Manning, and Prabhakar Raghavan. Introduction to information retrieval. Vol. 39. Cambridge University Press, 2008.